

Article

An Investigation of Vertically Distributed Aerosol Optical Properties over Pakistan Using CALIPSO Satellite Data

Miao Zhang ¹, Bo Su ^{1,2}, Muhammad Bilal ^{3,*}, Luqman Atique ⁴, Muhammad Usman ⁵, Zhongfeng Qiu ³, Md. Arfan Ali ³ and Ge Han ⁶

¹ School of Environmental Science and Tourism, Nanyang Normal University, Nanyang 473061, China; zm_liesmars@whu.edu.cn (M.Z.); subohappy@hhu.edu.cn (B.S.)

² School of Earth Sciences and Engineering, Hohai University, Nanjing 210098, China

³ School of Marine Sciences, Nanjing University of Information Science & Technology, Nanjing 210044, China; zhongfeng.qiu@nuist.edu.cn (Z.Q.); md.arfanali@nuist.edu.cn (M.A.A.)

⁴ School of Earth Sciences, Zhejiang University, Hangzhou 310027, China; lagondal@zju.edu.cn

⁵ Centre for Geographical Information System, University of the Punjab, Lahore 42000, Pakistan; muhammadusman.gis@pu.edu.pk

⁶ School of Remote Sensing and Information Engineering, Wuhan University, Wuhan 430079, China; udhan@whu.edu.cn

* Correspondence: muhammad.bilal@connect.polyu.hk; Tel.: +86-132-6085-6312

Received: 4 June 2020; Accepted: 7 July 2020; Published: 8 July 2020



Abstract: The vertically distributed aerosol optical properties are investigated over Pakistan utilizing the Cloud-Aerosol Lidar and Infrared Pathfinder Satellite Observation (CALIPSO) Level 2 products from 2007 to 2014. For a better understanding of the spatiotemporal characteristics of vertical aerosol layers, the interannual and seasonal variations of nine selected aerosol parameters such as the AOD of the lowest aerosol layer (AOD_L), the base height of the lowest aerosol layer (H_L), the top height of the highest aerosol layer (H_H), the volume depolarization ratio of the lowest aerosol layer (DR_L), the color ratio of the lowest aerosol layer (CR_L), total AOD of all the aerosol layers (AOD_T), the number of aerosol feature layers (N), the thickness of the lowest aerosol layer (T_L), the AOD proportion for the lowest aerosol layer ($PAOD_L$) for both day and night times are analyzed. The results show AOD_T increased slightly from 2007 to 2014 over Pakistan, and relatively high AOD_T exists over the Punjab and Sindh (southern region), which might be owing to the high level of economic development, frequent dust storms, and profound agricultural activities (anthropogenic emissions). AOD_T increases from north to south. The reason may be that the southern region is rapidly urbanized and is near the desert. The northern region is dominated by agricultural land, and cities are usually semi-urbanized. The highest AOD_T appears in summer compared to the other seasons, and during daytime compared to nighttime. The H_L and H_H vary significantly, owing to the topography of Pakistan. The N is relatively large over Punjab and Sindh compared to the other regions, which might be caused by relatively stronger atmospheric convections. The spatial distribution of the T_L showed an inverse relationship with the topography as lower values are observed over elevated regions such as Gilgit-Baltistan and Jammu-Kashmir. The value of the $PAOD_L$ indicates that 77% of the total aerosols are mainly concentrated in the lowest layer of the atmosphere over Pakistan. The higher values of DR_L and CR_L indicate non-spherical and large particles over Balochistan and Sindh, which might be related to the proximity to the desert. This study provides very useful information about vertically distributed aerosol optical properties which could help researchers and policymakers to regulate and mitigate air pollution issues of Pakistan.

Keywords: aerosols; CALIPSO; Pakistan; aerosol layers; AOD

1. Introduction

Atmospheric aerosols are composed of various solid or liquid particles suspended in the atmosphere with a particle size range of 10^{-3} – 10^2 μm [1–5]. They play an important role in the earth's radiation budget and global climate change [6,7]. Aerosols affect the climate through direct and indirect ways; i.e., aerosols directly change the radiation balance of the earth-atmosphere by absorbing and scattering the short-wave radiation of the sun and the long-wave radiation of the earth, thus affecting the global climate [8,9], and indirectly by altering the cloud microphysical characteristics and acting as cloud condensation nuclei (CCN). As the absorption and scattering of solar shortwave radiation by aerosol types is dissimilar, so the earth's radiation budget is influenced by various aerosol components [10–12]. In 2013, the fifth report of the Intergovernmental Panel on climate change (IPCC) pointed out that aerosols are one of the most uncertain factors affecting climate change [7]. In addition to the impact on climate change, aerosols are also related to environmental pollution events, such as the occurrence of photochemical smog, acid rain, smog weather, and haze, etc., [12–17]. At the same time, environmental pollution events also adversely affect human health, such as atherosclerosis, lung diseases, respiratory issues, and so on [18–20].

Because of the instability of aerosol space-time changes, the mechanism of its impact on the earth's radiation balance is complex and changeable, which limits our understanding of the climate system and global climate change. Therefore, it is necessary to continually study the long-term status of the space-time distribution of aerosol optical and physical properties to understand the aerosol-radiation interactions. At present, aerosol optical properties are mainly obtained from ground-based measurements and satellite-based observations. Ground-based measurements are conducted through Sunphotometers networks, such as the AEROSOL ROBOTIC NETWORK (AERONET), established by NASA, which provides continuous aerosol data globally [11,21,22]. Using high-resolution spectro-temporal datasets from AERONET, scientists have contributed to the knowledge gaps regarding aerosols [23–25]. However, because of the scattered geographical distribution of the AERONET sites and their limited spatial coverage, the large area and large scale characteristics of the aerosol cannot be obtained. Satellite observation can make up for the shortcomings of in situ observation, and help to achieve a large area and large-scale observations of aerosols around the globe. Aerosol research based on satellite remote sensing began in the mid-1970s. Advanced very high resolution radiometer (AVHRR) sensors on a series of polar-orbiting satellites of NOAA were used first time in aerosol remote sensing [26]. The availability of AVHRR marine aerosol remote sensing products became a valuable data source for aerosol researchers. With the availability of a world-wide high-frequency Moderate Resolution Imaging Spectroradiometer (MODIS), on Terra and Aqua satellites, sensor data, the monitoring of global aerosol optical properties has been realized [27–31]. In 2004, the Aura satellite launched by NASA, which carries the Ozone Monitoring Instrument (OMI) sensor of ozone observer, made available the aerosol index products which can help distinguish aerosol types [32,33]. On 28 April 2006, the Cloud-Aerosol Lidar and Infrared Pathfinder Satellite Observations (CALIPSO), jointly developed by NASA and CERES, was launched and became a member of A-train series of satellites [34–36].

CALIPSO is mainly used to study the three-dimensional distribution of physical and optical properties of clouds as well as aerosols at a global scale. CALIPSO data are of great significance to study the influence of clouds and aerosols on global radiation and make rather a precise parameterization of clouds and aerosols for improving modeling knowledge about climate, weather forecast, air quality, and related models. CALIOP (Cloud-Aerosol Lidar with Orthogonal Polarization), one of the payloads of the CALIPSO satellite [37], is an active optical sensor, with dual-wavelength polarization-sensitive channels with unique advantages: Long-term continuous and high-precision monitoring; it can operate by day and night; it can observe the thin clouds as well as the multi-layer structure of clouds and aerosols, which is the only technology currently available to accurately observe the thin clouds and aerosol profiles simultaneously [38]. It would help researchers to further explore knowledge about aerosols and clouds and to study the global climate and temperature changes.

In Asia, because of developments in the economy, urbanized and industrialized areas are constantly increasing, resulting in the growth of anthropogenic emissions and aerosol loadings in the atmosphere. Pakistan enjoys a topography hosting mountains and plains, with a subtropical climate. Pakistan is one of the most polluted countries in Asia [39] and so far, relatively few studies related to aerosol optical properties have been conducted over Pakistan using passive remote sensing satellites such as MODIS [23] and OMI [40]. Gohar et al. [41] investigated trends in AOD using long-term data derived from MODIS over twelve regions in Pakistan. Salman et al. [42] analyzed the aerosol index deduced from OMI over Pakistan from December 2004 to November 2008 and found that the aerosol index value in Pakistan had significant spatio-temporal changes, with higher values in southern parts of Pakistan and lower values in the northern parts. Shahid et al. [43] have shown that coal-fired power plants in India are a major source of cross-border air pollution affecting northeast Pakistan, and aerosol concentrations in South Asia show a minimum during the monsoon season (June–September) and a maximum during the post-monsoon season (October–November). The accurate assessment of the aerosol effects on climate as well as urban air quality depends on the precise and systematic understanding of the physical, chemical, and optical properties of aerosols as well as their spatiotemporal and vertical distributions. To our best knowledge, no single study has been conducted previously related to vertical distributions of different aerosol layers for both day and night times over Pakistan. Therefore, by taking advantage of this opportunity, for the first time, this study analyzed the vertical distributions of aerosol optical characteristics over Pakistan for both day and night times using the CALIOP Level-2 aerosol layers product from 2007 to 2014.

2. Methodology

2.1. Study Area

Figure 1 shows the geographical distribution of Pakistan with respect to elevation. Pakistan is situated in the northwest of the South Asian subcontinent, bordering the Arabian Sea in the south, and neighboring India, China, Afghanistan, and Iran in the East, North, and West, respectively. The coastline is 840 km long. Three-fifth of the land area is mountainous and hilly, the southern region is desert and coastline, and the northward extension is continuous plateau pasture and fertile land. The highest peak in the country is the Gorgory peak (8611 m above sea level). Three famous mountains in the world; i.e., Himalayas, Karakoram, and the Hindu Kush, converge in the northeast of Pakistan. Pakistan's annual temperature (27 °C) is generally high, and the precipitation is relatively low. The area with annual precipitation less than 250 mm accounts for more than three-quarters of the total area of the country. Pakistan has a subtropical climate with humid and hot in the south, affected by monsoon, dry and cold in the north, with snow all-year-round in some places [23,44].

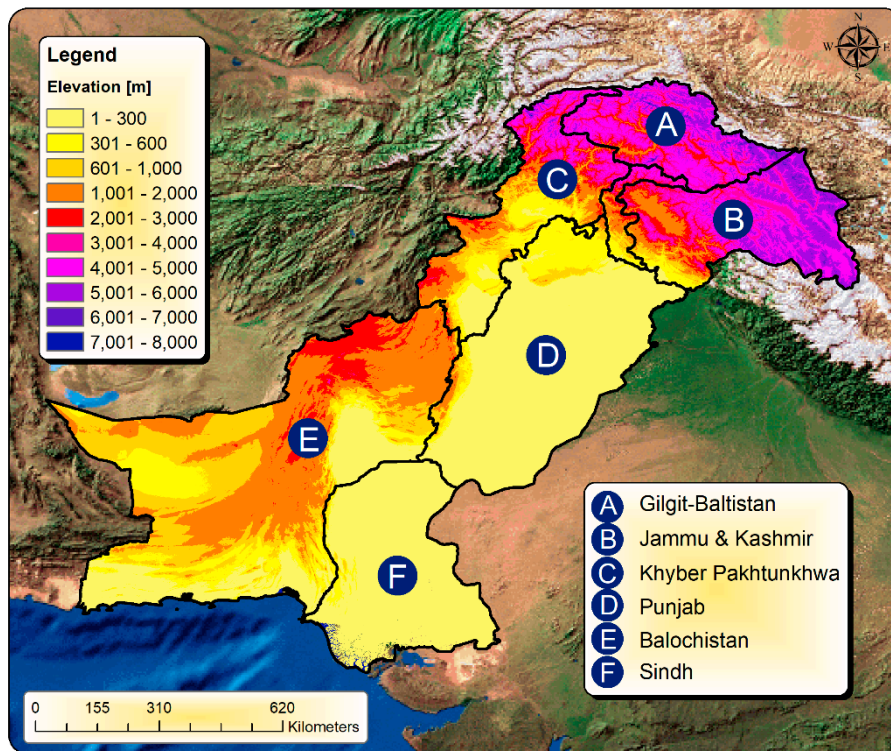


Figure 1. Geographical locations of Pakistan. The color variations represent elevation.

2.2. Materials and Methods

The CALIOP lidar is one of the main payloads of the CALIPSO satellite, a solar synchronous polar orbit satellite, with an orbital altitude of 705 km, an orbit speed of 7 km/s, a circle around the earth every 96 min, and a repeat coverage time of 16 days. CALIOP is a dual-wavelength orthogonal polarization lidar, which consists of a laser transmitting and receiving subsystems. In the emission system, the laser can generate 532 nm and 1064 nm laser pulses at the same time. The pulse energy is about 110 mJ, and the pulse repetition frequency is 20.16 Hz. The laser emits signals approximately vertically on the earth's surface, forming a spot with a diameter of about 70 m and a horizontal interval of 333 m. There are three receiving channels in the receiving system, which receive 1064 nm backscatter signal and 532 nm backscatter signal. CALIOP data are available three levels and Level 2 (L2) data are used in this paper. The L2 data can be divided into three types: (a) Cloud and aerosol layers data product (Clay/Alay), which provides the number of cloud/aerosol layers, top height, layer optical thickness, etc.; (b) cloud and aerosol vertical profile data (CPro/APro), which provides the vertical distribution backscatter coefficient and extinction coefficient; (c) the vertical feature mask (VFM) data product, which provides the classification information of detectable features (cloud and aerosol) [38].

The data employed have a horizontal resolution of 5 km. To better analyze the vertical optical and physical characteristics of the aerosol layers, the characteristics of all aerosol layers are analyzed together, and the lowest aerosol layer individually. In this study, the parameters used are the AOD of the lowest aerosol layer (AOD_L), the top height of the lowest aerosol layer (H_L), the top height of the highest aerosol layer (H_H), the volume depolarization ratio of the lowest aerosol layer (DR_L), the color ratio of the lowest aerosol layer (CR_L), total AOD of all the aerosol layers (AOD_T), the number of aerosol feature layers (N), the thickness of the lowest aerosol layer (T_L), the AOD proportion for the lowest aerosol layer ($PAOD_L$). AOD_L , H_L , H_H , DR_L , CR_L , N can be obtained directly from L2 data, whereas, AOD_T , T_L , and $PAOD_L$ were obtained by indirect calculations using the following Equations [45]:

$$AOD_T = \sum_1^N AOD_N; N = 1, 2, \dots, 7, 8 \quad (1)$$

where, $N = 1$ represents the lowest aerosol layer; i.e.,

$$\text{AOD}_L = \text{AOD}_1 \quad (2)$$

$$T_L = H_L - B_L \quad (3)$$

where, B_L represents the base height of the lowest aerosol layer and can be obtained directly from L2 data;

$$\text{PAOD}_L = \frac{\text{AOD}_L}{\text{AOD}_T} \times 100\% \quad (4)$$

To infer a detailed picture of the temporal and spatial variation characteristics of aerosols in Pakistan, it has been divided into six regions, namely A: Gilgit-Baltistan; B: Jammu-Kashmir; C: Khyber-Pakhtunkhwa; D: Punjab; E: Balochistan; and F: Sindh. The annual and seasonal statistical information of several aerosol variables over these six regions is calculated from 2007 to 2014 to reveal the annual and seasonal changes in the aerosol properties over Pakistan. In this study, null values and values less than or equal to zero were eliminated and the remaining data were re-sampled to $1^\circ \times 1^\circ$ grid. For this purpose, this study has utilized both day and night times cloud-free images. The clouds (both thick and thin) were discriminated by the Selective Iterated Boundary Locator (SIBYL) and Scene Classification Algorithms (SCA) [35]. The SIBYL algorithm can also calculate every backscatter profile of CALIOP to identify the aerosol feature layers, and when the backscatter value is beyond the threshold value, then the existence of aerosol feature layers is recognized as one. The whole number of aerosol feature layers in one backscatter profile can be defined as the N values. In this study, CALIPSO overpass tracks; i.e., 5 for daytime and 5 for nighttime, were analyzed over Pakistan [36].

3. Results and Discussion

3.1. Interannual Variations in Optical Characteristics of Aerosol Layers

Annual mean values of AOD_T have been analyzed from 2007 to 2014 over Gilgit-Baltistan, Jammu-Kashmir, Khyber-Pakhtunkhwa, Punjab, Balochistan, and Sindh. Figure 2a (for daytime) and Figure 3a (for nighttime) demonstrate that the annual mean AOD_T is slightly increased over Pakistan, which can be associated with the economic development, industrial activity, and agricultural and dust storm activities. This result is similar to that of Gohar et al. [41], who analyzed the AOD annual average variation trend of 12 regions in Pakistan by using MODIS in 15 years (2003–2017), and the AOD generally presents an increasing trend of annual variation. Since the world over the subprime crisis in 2008, the economic development of Pakistan also suffered a relative slow down. In comparison with other Asian countries, aerosol concentrations did not increase significantly between 2007 and 2014. The annual mean values of AOD_T were higher over Sindh (daytime: 0.52, nighttime: 0.46) and Punjab (daytime: 0.49, nighttime: 0.50), followed by Balochistan (daytime: 0.41, nighttime: 0.36), Khyber-Pakhtunkhwa (daytime: 0.36, nighttime: 0.28), Jammu-Kashmir (daytime: 0.26, nighttime: 0.18), and Gilgit-Baltistan (daytime: 0.17, nighttime: 0.09). Punjab and Sindh are Pakistan's leading provinces as well as the first and second-largest regional economies, respectively, therefore, this can be a reason for higher AOD over these two regions compared to the other regions. In the Southeast of Pakistan, the Thar desert contributes to the higher annual mean AOD values over the bordering eastern provinces of Punjab and Sindh compared to the other four regions. Shahid et al. [43] pointed out that some observational analysis had proved the importance of aerosol transport from northern India. Indian coal-fired power plants are the main source of cross-border air pollution affecting northeast Pakistan [46]. Another persuasive reason might be that aerosols from multiple sources such as industrial emissions, vehicle emissions, and locally generated dust are mixed to increase the AOD values, [44,47]. Overall, the annual mean AOD_T values are slightly higher (~ 0.1) during the daytime compared to the nighttime, which could effectively be related to the higher frequency of human activities during daytime than nighttime, resulting in the higher anthropogenic aerosol emissions.

The results show higher annual mean values of N over Punjab (daytime: 2.32, nighttime: 2.41) and Sindh (daytime: 2.30, nighttime: 2.20), sequentially succeeded by Balochistan (daytime: 1.93, nighttime: 1.94), Khyber-Pakhtunkhwa (daytime: 1.78, nighttime: 1.93), Jammu-Kashmir (daytime: 1.48, nighttime: 1.63), and Gilgit-Baltistan (daytime: 1.07, nighttime: 1.43) (Figures 2b and 3b). It is also evident from Figure 4 (for daytime) and Figure 5 (nighttime) that the spatial distributions of N values are greater than 2 over Punjab and Sindh (low elevated terrain as shown in Figure 1) compared to the other regions (moderate to high elevated terrain). A plausible reason could be that these two regions geographically stretched toward the southern part of Pakistan with relatively high temperatures, strong vertical movement of the atmosphere, as well as bearing large atmospheric aerosol load, resulting in the obvious vertical stratification of the atmosphere. Besides, the values in Punjab are higher than those in Khyber-Pakhtunkhwa and Balochistan along similar latitudes, which might be ascribed to the mountainous terrain of Khyber-Pakhtunkhwa and Balochistan, characterized by lower temperatures, relatively weaker vertical convection, and low aerosol load. Thus, the vertical stratification of atmospheric aerosols is relatively weak, resulting in the low N values. Overall, these results suggested that the number of aerosol layers (N) shows variations with respect to terrain pattern; i.e., N is higher over the low-elevated terrain compared to the moderate to high elevated terrain.

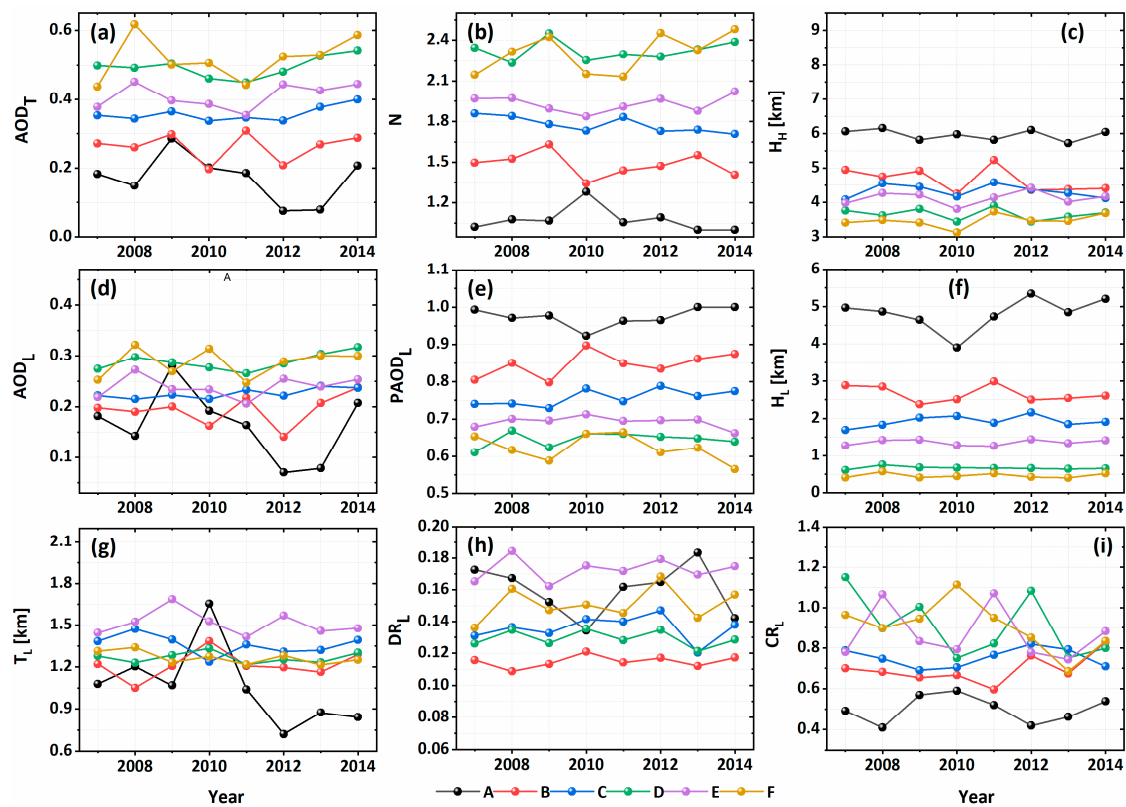


Figure 2. Interannual variations in the optical characteristics of aerosol layers over Pakistan (A: Gilgit-Baltistan, B: Jammu-Kashmir, C: Khyber-Pakhtunkhwa, D: Punjab, E: Balochistan, F: Sindh) during daytime from 2007 to 2014. (a) the AOD of all the aerosol layers (AOD_T), (b) the AOD of the lowest aerosol layer (AOD_L), (c) the top altitude of the lowest aerosol layer (H_L), (d) the top altitude of the highest aerosol layer (H_H), (e) the number of aerosol feature layers (N), (f) the thickness of the lowest aerosol layer (T_L), (g) the AOD proportion of the lowest aerosol layer ($PAOD_L$), (h) the volume depolarization ratio of the lowest aerosol layer (DR_L), and (i) the color ratio of the lowest aerosol layer (CR_L).

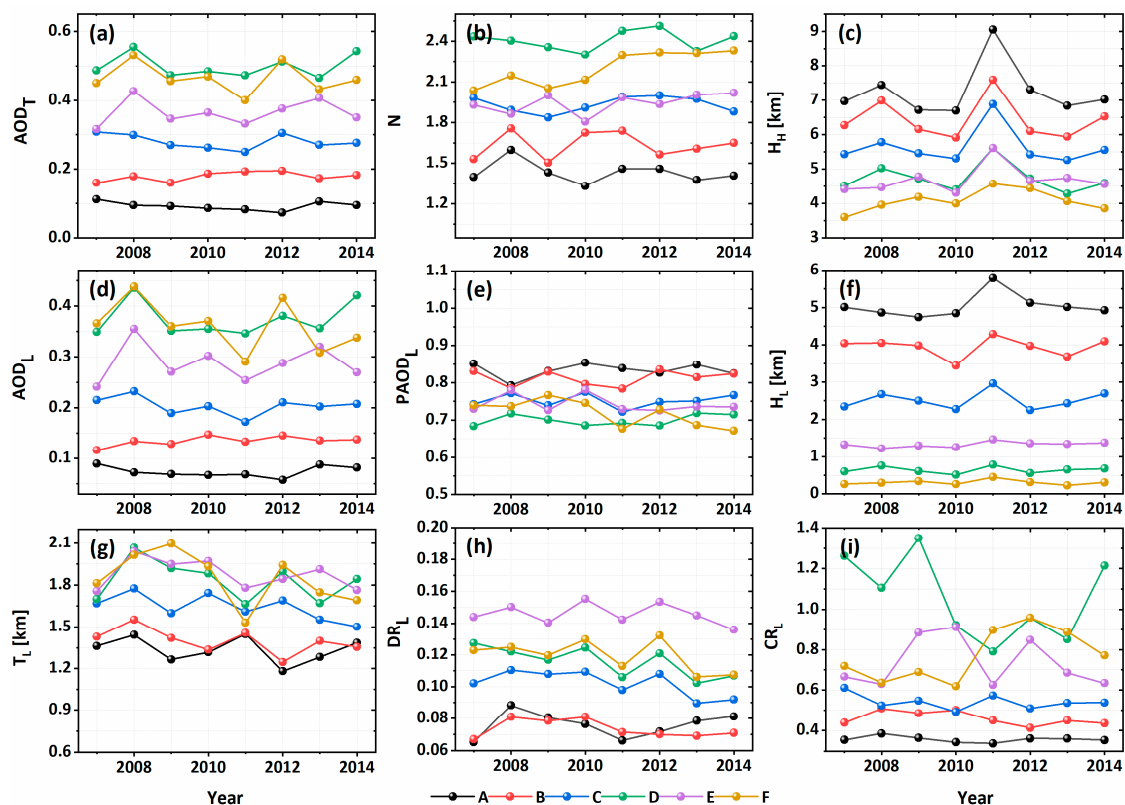


Figure 3. Interannual variations in the optical characteristics of aerosol layers over Pakistan (A: Gilgit-Baltistan, B: Jammu-Kashmir, C: Khyber-Pakhtunkhwa, D: Punjab, E: Balochistan, F: Sindh) during nighttime from 2007 to 2014. Where, (a) AOD_T , (b) AOD_L , (c) H_L , (d) H_H , (e) N , (f) T_L , (g) $PAOD_L$, (h) DR_L , and (i) CR_L .

The annual mean values of H_L and H_H were higher over Gilgit-Baltistan, followed by Jammu-Kashmir, Khyber-Pakhtunkhwa, Balochistan, Punjab, and Sindh (Figures 2c,f and 3c,f). These results indicate that H_L and H_H have a clear relationship with the terrain pattern; i.e., the higher the altitude of a geographic location, the greater the values of H_L and H_H over the region. Similarly, higher the values of H_L and H_H (or elevation of the terrain), the low aerosol loadings in the atmosphere [48]. The inverse relationship between elevation and aerosol loadings was also reported over the hilly terrain of Hong Kong by Bilal et al. [49]. Therefore, these results also suggest that aerosol particles exist at lower altitudes over Sindh and Punjab which may have more impacts on human health, air quality, and local weather conditions, especially in some large and densely populated cities such as Lahore, Okara, Faisalabad, Mirpur Khas, Sukkur, and Shikarpur.

AOD_L is the AOD value of the lowest aerosol layer, which is greatly affected by both natural and anthropogenic activities. Annual mean values of AOD_L (Figures 2d and 3d) present a similar annual change pattern as AOD_T ; i.e., higher values over Punjab (daytime: 0.29, nighttime: 0.37) and Sindh (daytime: 0.29, nighttime: 0.36) followed by Balochistan (daytime: 0.24, nighttime: 0.29), Khyber-Pakhtunkhwa (daytime: 0.23, nighttime: 0.20), Jammu-Kashmir (daytime: 0.19, nighttime: 0.13), and Gilgit-Baltistan (daytime: 0.16, nighttime: 0.07). Interestingly, AOD_L is higher during nighttime compared to the daytime over Punjab, Sindh, and Balochistan and for this, meteorological factors such as boundary layer height, wind speed, and ventilation coefficient may be responsible. In general, the nocturnal boundary layer is shallower compared to the daytime, and the ventilation coefficient, which represents atmospheric dispersion and calculated by boundary layer height multiplied with wind speed, rapidly decreases because of low wind speed. This phenomenon confines the aerosols at the lowest aerosol layer during nighttime compared to the daytime [50].

PAOD_L represents the AOD proportion for the lowest aerosol (Figures 2e and 3e). The results reveal the rank of the large percentage of PAOD_L over Gilgit-Baltistan (daytime: 94%, nighttime: 78%) > Jammu-Kashmir (daytime: 73%, nighttime: 72%) > Khyber-Pakhtunkhwa (daytime: 64%, nighttime: 71%) > Balochistan (daytime: 59%, nighttime: 81%) > Punjab (daytime: 59%, nighttime: 74%) > Sindh (daytime: 56%, nighttime: 78%). Although a large percentage of PAOD_L was observed over the elevated region, aerosol loadings over these regions are less vulnerable to human health because of the high altitude of the lowest aerosol layer (H_L) as well as less aerosol loadings. Also, Gilgit-Baltistan and Jammu-Kashmir are mountainous regions with relatively low temperature, therefore, the number of aerosol layers (N) is less over these regions due to weak atmospheric stratification. This indicates that the number of all the aerosol layers might be equal to the lowest aerosol layer, and it can be the possible reason for the large percentage of PAOD_L over these regions. However, a large percentage of PAOD_L during nighttime comparable to daytime is more vulnerable to human health in Punjab and Sindh because of the significant aerosol loadings at the lowest aerosol layer (AOD_L) as well as the low altitude of the lowest aerosol layer (H_L).

T_L is the difference between the top height of the lowest aerosol layer (H_L) and the base height of the lowest aerosol layer (B_L). The results show that the annual mean values of T_L (Figures 2g and 3g) over Khyber-Pakhtunkhwa (daytime: 1.36 km, nighttime: 1.64 km), Punjab (daytime: 1.27 km, nighttime: 1.83 km), Balochistan (daytime: 1.51 km, nighttime: 1.88 km), and Sindh (daytime: 1.27 km, nighttime: 1.85 km) are slightly higher than Gilgit-Baltistan (daytime: 1.06 km, nighttime: 1.34 km), and Jammu-Kashmir (daytime: 1.21 km, nighttime: 1.40 km) vary during the day and night times, and relative large values are observed during nighttime compared to the daytime.

DR_L is the ratio of the vertical polarization scattering coefficient at 532 nm to the whole aerosol scattering coefficient at 532 nm, which reflects the spherical and non-spherical degree of aerosol particles in the lowest aerosol layers. The smaller values of DR_L represents more spherical aerosol particles and vice versa. The results show highest values of the annual mean DR_L over Balochistan (daytime: 0.17, nighttime: 0.15) and Sindh (daytime: 0.15, nighttime: 0.12) compared to Punjab (daytime: 0.13, nighttime: 0.12), Gilgit-Baltistan (daytime: 0.16, nighttime: 0.08), and Jammu-Kashmir (daytime: 0.11, nighttime: 0.07) (Figures 2h and 3h). These results suggest the presence of more non-spherical particles over Balochistan and Sindh, as these regions are mainly affected by dust particles. These results also suggest the presence of more non-spherical particles during the daytime compared to the nighttime, which might be due to dry deposition during the nighttime compared to the daytime.

The color ratio is the ratio between the total attenuation backscattering coefficient of 1064 nm and the total attenuation backscattering coefficient of 532 nm. It represents the particle size of the measured particles, and the higher the color ratio, the larger the particle size [45]. Figures 2i and 3i depict the annual mean variation of the CR_L in the lowest aerosol layer during daytime and nighttime, which reflects the size of the aerosol particles; i.e., higher the values of CR_L, the larger the aerosol particle size. The results show higher values of CR_L over Punjab (daytime: 0.91, nighttime: 1.06), Balochistan (daytime: 0.87, nighttime: 0.74), and Sindh (daytime: 0.90, nighttime: 0.77) compared to Gilgit-Baltistan (daytime: 0.50, nighttime: 0.52), Jammu-Kashmir (daytime: 0.70, nighttime: 0.46), and Khyber-Pakhtunkhwa (daytime: 0.75, nighttime: 0.54). These results suggest the presence of more coarse-mode (large size particles) over Punjab, Balochistan, and Sindh, and this might be due to the reason that the aerosols are mainly of sand and dust type, being in the proximity of the desert, which results in the high CR_L values in southern Pakistan.

3.2. Seasonal Variation Characteristics of the Aerosol Layers over Pakistan

We also performed seasonal analyses to investigate the vertical distributions of aerosols optical characteristics during the day and night times (Figures 4–7). The seasons are defined as spring (March to May), summer (June to August), autumn (September to November), and winter (December to February). AOD_T values (Figures 6a and 7a) reached the highest values in summer (daytime: 0.61, nighttime: 0.46) and the lowest in winter (daytime: 0.24, nighttime: 0.22), which is consistent with the

results of various researches. Shahid et al. [43] found that particulate concentrations in northeastern Pakistan were linked to anthropogenic emissions and meteorological factors. Through the PM data in 2006, it was found that the concentration of particulate matter was closely related to temperature and precipitation. In October, low precipitation and low temperature lead to a high concentration of particulate matter. Ranjan et al. [51] found that the lowest mean AOD values occur from October to December. Sarkar et al. [52] found that AOD starts to increase from March and reaches the maximum in June over India, however, a high AOD persists over neighboring Pakistan and the Arabian Sea until August. The air masses travel far to Pakistan in winter and near in summer. The high AOD value in summer is closely related to the long residence time of air masses [41,47]. The higher values in summer could be attributed to the higher temperature, which plays an important role in heating and promoting the loose material in the soil, as well as attributed by frequent dust storms activates [44,52,53]. Besides, the water vapor content is directly related to the AOD load in the atmosphere [54]. The higher the water vapor concentration in summer, the higher the relative humidity of the atmosphere, in turn, the higher the AOD [12,55]. The lower values in winter (winter monsoon) could be due to less or no dust storm activities [56]. As can be seen from the spatial distributions map (Figures 4 and 5), AOD values over the Punjab and Sindh, in summer, are relatively high compared to other regions, especially in large urban places such as Lahore, Rohri, and Karachi. These results indicate that the AOD values are related to levels of economic development, urbanization, population, automobiles emissions, and dust storms, which is consistent with the results of Gohar Ali et al. [41]. Notably, the seasonal variation in AOD_L values is consistent with the long-term spatial and temporal distributions of mean AOD_L over six regions of Pakistan (Figures 6d and 7d). Tariq et al. [42] used ozone monitoring instrument (OMI) to conduct remote sensing research on the absorptive aerosol of Pakistan from 2004 to 2008, and found that the aerosol index of Pakistan was higher in the south than in the north, with the maximum value appearing in May and the minimum value appearing in December. The results are consistent with those in this paper [42].

The seasonal mean values of N over Gilgit-Baltistan and Jammu-Kashmir have a slight difference in four seasons (Figures 6b and 7b). The highest values of N were observed over the other four regions during the daytime in summer (2.37), while, values decreased at night time from 2.32 to 1.99 from spring to winter, respectively. This might be due to the higher temperatures in spring and summer and the enhancement of vertical convection, which consequently results in the stratification of aerosols. The seasonal mean N values over Punjab (daytime: 2.27, nighttime: 2.41) and Sindh (daytime: 2.28, nighttime: 2.19) are higher than that over Balochistan (daytime: 1.92, nighttime: 1.91), Khyber-Pakhtunkhwa (daytime: 1.79, nighttime: 1.92), Jammu-Kashmir (daytime: 1.48, nighttime: 1.65), and Gilgit-Baltistan (daytime: 1.12, nighttime: 1.42). According to the spatial distribution maps (Figures 4 and 5), the high values of N are mainly distributed over the big urban areas of Punjab and Sindh, characterized by the relatively high economic activities, dense population, higher presence of industrial units, intense agricultural practices, enhanced automobile exhaust emissions, and prompting higher emissions of pollutants into the atmosphere.

As can be seen from the spatial distribution maps (Figures 4 and 5), the higher the geographic elevation, the greater the seasonal mean values of H_L. In comparison with H_L, the seasonal mean values of H_H did not much vary over the regions (Figures 6c and 7c). The high values of H_L are observed over Gilgit-Baltistan, Jammu-Kashmir, Khyber-Pakhtunkhwa, Balochistan, Punjab, and Sindh. The results depict a gradual decreasing seasonal trend from spring to winter. The trends in H_H values are similar to the H_L variation, which is plausibly due to the enhancement of vertical convection, caused by a seasonal temperature gradient, resulting in the heightening of the aerosol layer vertical movements. Besides, the values of H_H are higher (~2 km) during the day than the night, which might be due to the residual aerosols transported toward the higher altitudes during the day with the increased solar heating [47]. The seasonal mean values of H_L are higher in spring and summer than in autumn and winter for the five regions: Jammu-Kashmir, Khyber-Pakhtunkhwa, Punjab, Balochistan, and Sindh, and reached the highest in summer (daytime: 2.11 km, nighttime: 2.94 km). The seasonal

mean HB_1 was the highest over Gilgit-Baltistan (daytime: 4.90 km, nighttime: 4.95 km), followed by Jammu-Kashmir (daytime: 2.75 km, nighttime: 3.91 km), Khyber-Pakhtunkhwa (daytime: 1.89 km, nighttime: 2.56 km), Balochistan (daytime: 1.37 km, nighttime: 1.41 km), Punjab (daytime: 0.73 km, nighttime: 0.67 km), and Sindh (daytime: 0.57km, nighttime: 0.45 km), which might be due to topography enjoyed by the respective regions (Figures 6f and 7f) as well as deeper and shallower boundary layers, respectively.

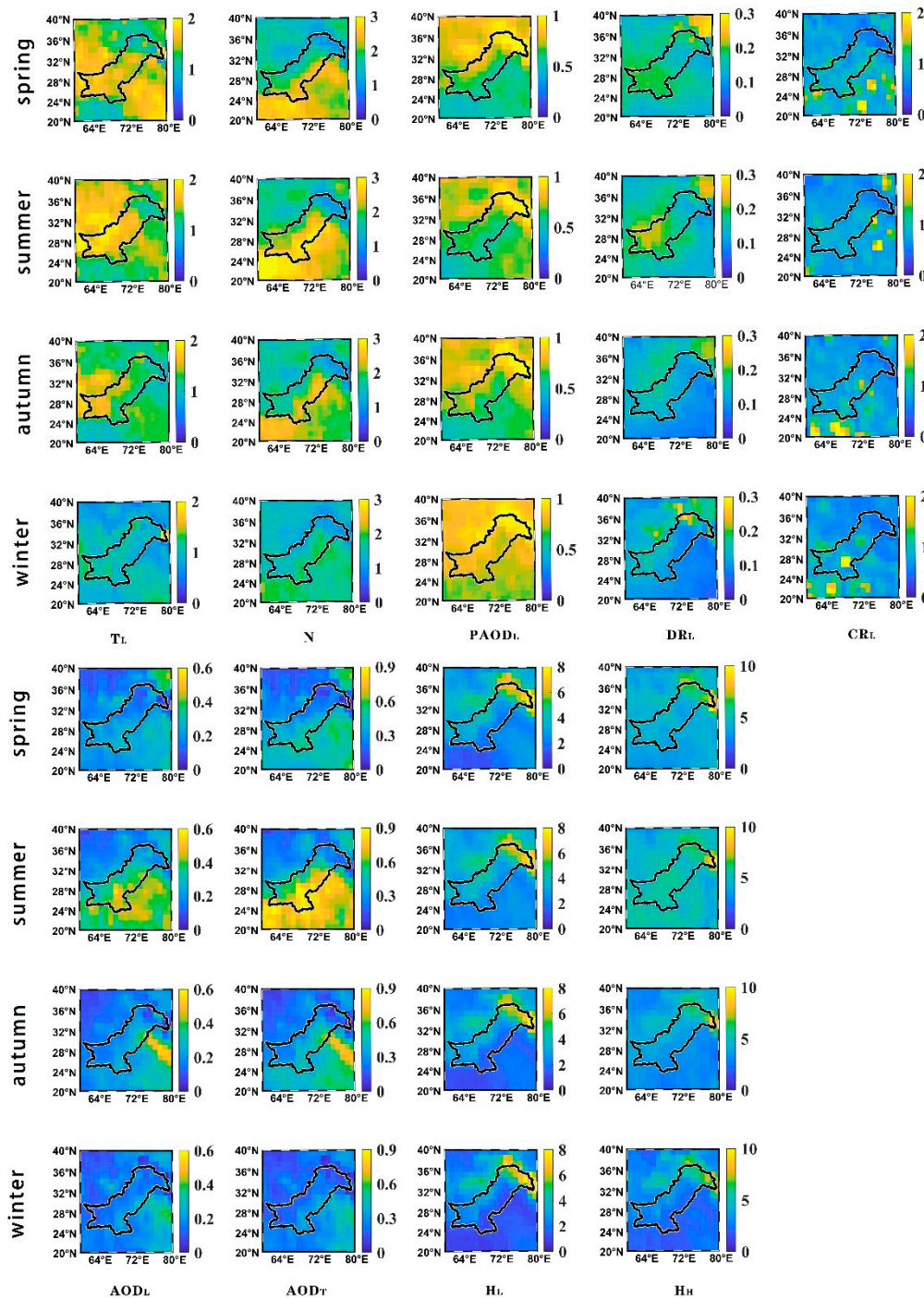


Figure 4. Seasonal spatial distributions of AOD_T , AOD_L , H_L , H_H , N , T_L , $PAOD_L$, DR_L , and CR_L over Pakistan during the daytime.

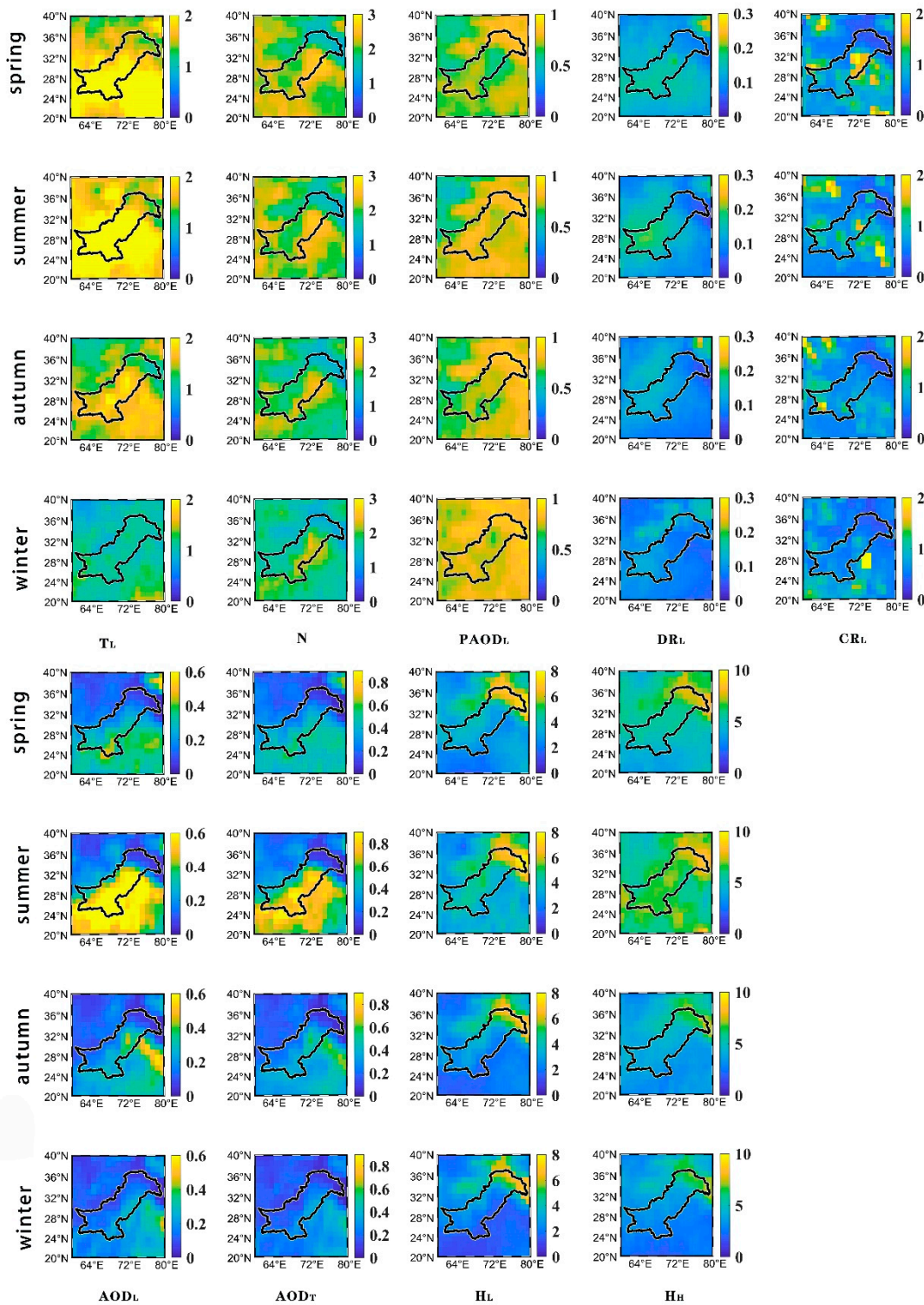


Figure 5. Seasonal spatial distributions of AOD_T , AOD_L , H_L , H_H , N , T_L , $PAOD_L$, DR_L , and CR_L over Pakistan during the nighttime.

The mean percentage of $PAOD_L$ for all the seasons together is almost the same for all the regions (daytime: 79%, nighttime: 73%) (Figures 6e and 7e). The percentages are slightly higher in winter compared to the other seasons, which might be related to the variational character exhibited by AOD_T (AOD_L) and N as discussed above. Besides, $PAOD_L$ values are higher (~2%) during the day than the night, this might be due to more aerosol loadings in the lowest aerosol layer dominated by coarse mode

aerosols (dust particles). The seasonal mean values of T_L in spring and summer (daytime: 1.42 km, nighttime: 2.00 km) are higher than those in autumn and winter (daytime: 1.19 km, nighttime: 1.41 km). As T_L is computed from H_L and H_H , therefore, its variation mainly depends on the distributions of H_L and H_H (Figures 6g and 7g). Also, the T_L values at night are slightly higher (~1 km) than those observed during the day.

The seasonal mean values of DR_L are higher in spring and summer (daytime: 0.17, nighttime: 0.12) than in autumn and winter (daytime: 0.14, nighttime: 0.10), which might be owing to the relatively severe dust transport in these two seasons [57], resulting in the strong aspheric feature of the aerosols (Figures 6h and 7h). The seasonal mean values of DR_L for Balochistan, Sindh, and Punjab are higher than Khyber-Pakhtunkhwa, Gilgit-Baltistan, and Jammu-Kashmir.

The seasonal mean values of CR_L did not change significantly during the four seasons (daytime: 0.77, nighttime: 0.66), however, it exhibits a gradual increase from north to south in spatial distribution, as, most likely, the southern region is close to a vast desert area, injecting higher sand dust in the atmosphere, hence, relatively high CR_L values caused by the large size of sand particles (Figures 6i and 7i).

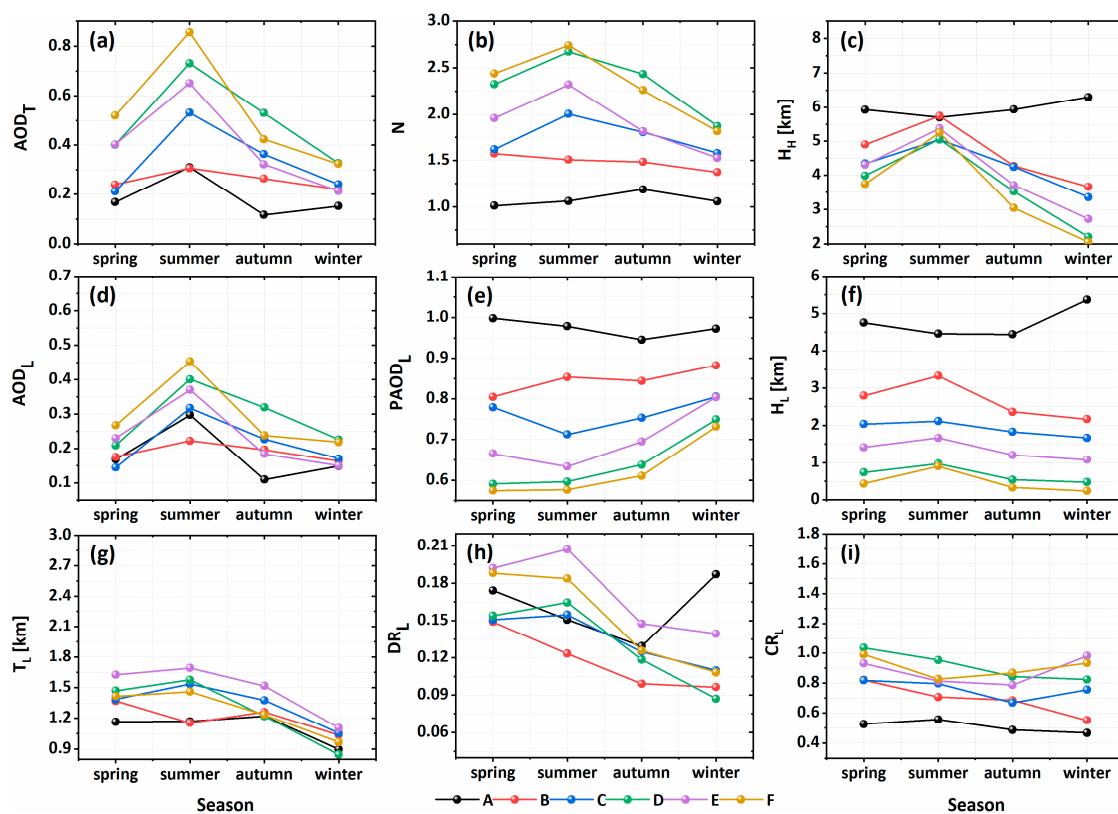


Figure 6. Seasonal variations in the optical characteristics of aerosol layers over Pakistan (A: Gilgit-Baltistan, B: Jammu-Kashmir, C: Khyber-Pakhtunkhwa, D: Punjab, E: Balochistan, F: Sindh) during daytime from 2007 to 2014. (a) AOD_T , (b) AOD_L , (c) H_H , (d) H_L , (e) N , (f) T_L , (g) $PAOD_L$, (h) DR_L , and (i) CR_L .

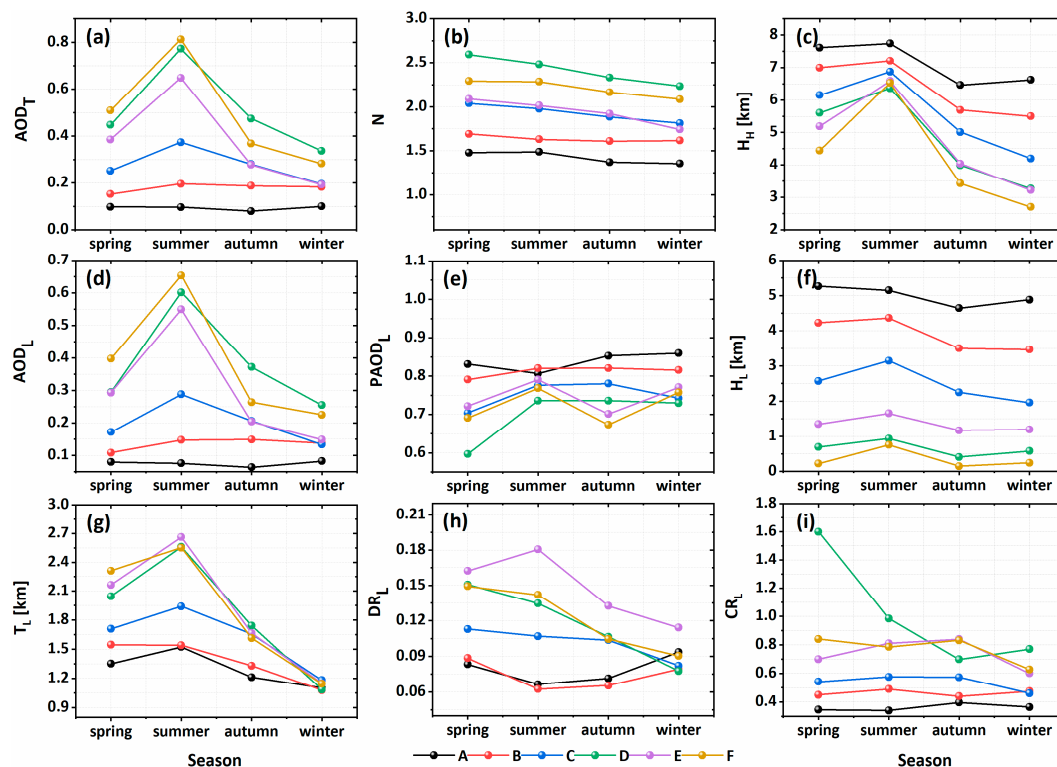


Figure 7. Seasonal variations in the optical characteristics of aerosol layers over Pakistan (A: Gilgit-Baltistan, B: Jammu-Kashmir, C: Khyber-Pakhtunkhwa, D: Punjab, E: Balochistan, F: Sindh) during nighttime from 2007 to 2014. (a) AOD_T , (b) AOD_L , (c) H_L , (d) H_H , (e) N , (f) T_L , (g) $PAOD_L$, (h) DR_L , and (i) CR_L .

3.3. The Correlation of Aerosol Properties over Pakistan

To better understand the spatiotemporal distributions of aerosols characteristics over Pakistan, seasonal correlation analysis among some parameters of the vertical aerosol layers was performed (Figure 8). Results show weak to a strong positive correlation between AOD_L and T_L which varies from season to season as well as region to region. This is similar to the situation in the Qinghai-Tibet Plateau and the western Yellow River Basin [31,45,58]. The higher positive correlation was observed in summer, compared to the other seasons, over all the regions except over Gilgit-Baltistan. In summer, the higher correlation was observed over Punjab, Sindh, and Balochistan as the aerosol concentrations over these regions are relatively higher compared to the other regions. The higher positive correlation indicates the more aerosol loadings in the lowest layer is directly related to the thickness of the lowest aerosol layers. This result is supported by a previous study [23] that reported a significantly higher value of AOD (~ 0.70) for the 15 years over Punjab compared to the other regions.

Figure 9 depicts the correlation between N and H_H over Pakistan. Because of less stratification over the three regions A, B, and C, especially over A, where the maximum value of N does not exceed 3, resulting in an inconspicuous positive linear correlation between N and H_H . The maximum value of N over D, E, and F is ~ 7 , which has a strong positive correlation ~ 7 with H_H . These phenomena reveal that the higher the H_H , the larger the N values in most cases. These results are consistent with the existing knowledge and the reported results for the Yellow River Basin and the Qinghai Tibet Plateau [45,58].

The correlation between N and $PAOD_L$ (Figure 10) for the entire six regions of Pakistan reveals that the two parameters demonstrate a significant negative correlation. Except for region A, which experiences less stratification, and correlation in the other five regions is greater than -0.9 . Since $PAOD_L$ refers to the proportion of AOD of the lowest aerosol layer, and theoretically, a large number of layers (N) leads to the smaller values of $PAOD_L$, and these results are supported by the previous studies [45,58].

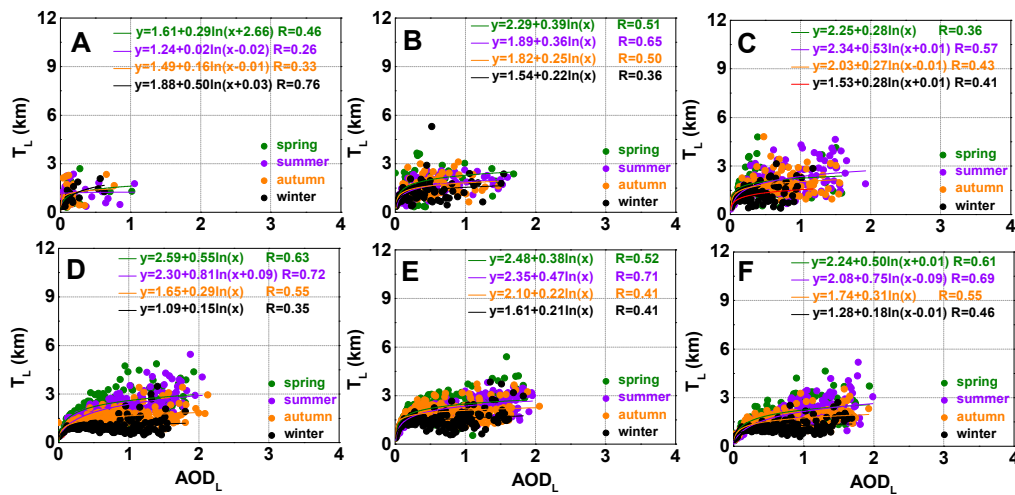


Figure 8. Correlation between AOD_L and T_L over Pakistan (A: Gilgit-Baltistan, B: Jammu-Kashmir, C: Khyber-Pakhtunkhwa, D: Punjab, E: Balochistan, F: Sindh) from 2007 to 2014.

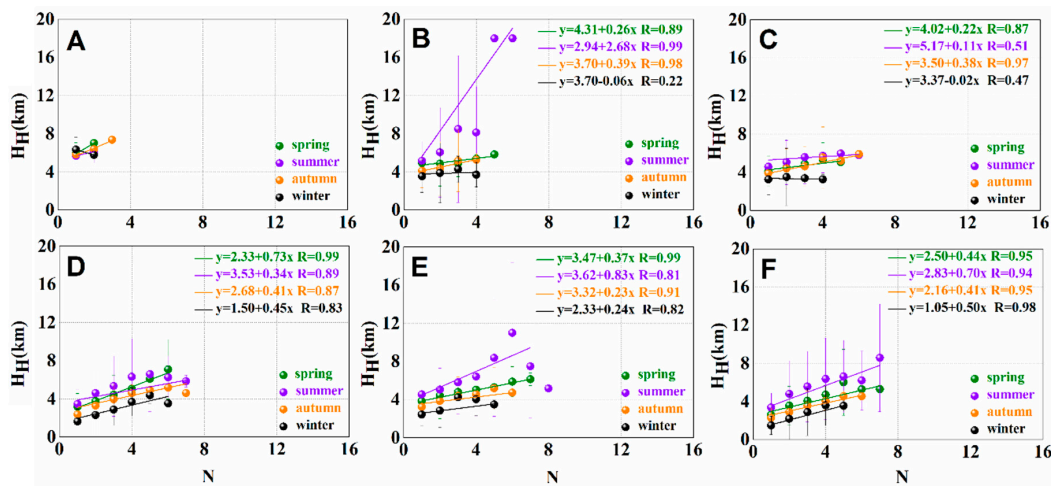


Figure 9. Correlation between N and H_H over Pakistan (A: Gilgit-Baltistan, B: Jammu-Kashmir, C: Khyber-Pakhtunkhwa, D: Punjab, E: Balochistan, F: Sindh) from 2007 to 2014.

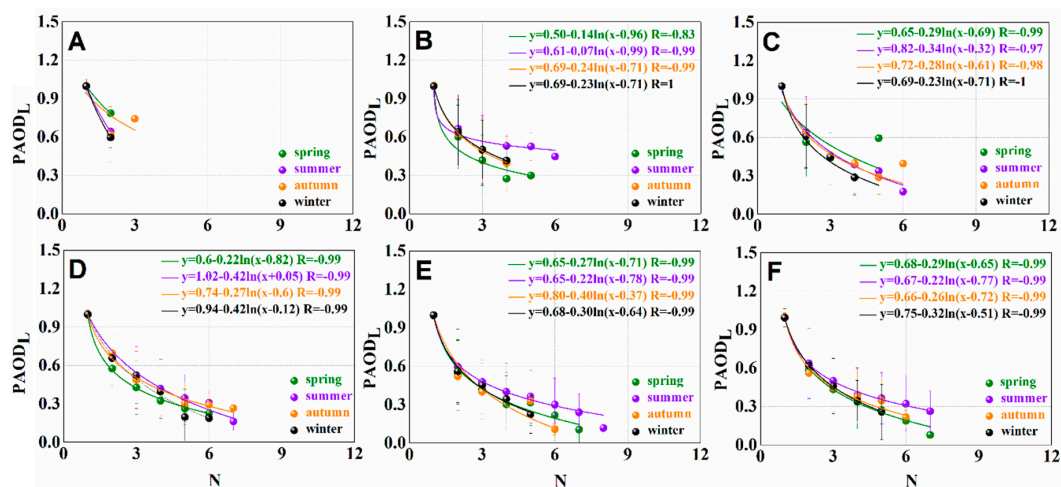


Figure 10. Correlation between N and PAOD_L over Pakistan (A: Gilgit-Baltistan, B: Jammu-Kashmir, C: Khyber-Pakhtunkhwa, D: Punjab, E: Balochistan, F: Sindh) from 2007 to 2014.

4. Conclusions

In this study, the spatiotemporal optical characteristics of the vertical aerosol layers were investigated over Pakistan using CALIPSO Level-2 aerosol layers product from 2007 to 2014. The interannual and seasonal variations of AOD_T , AOD_L , H_L , H_H , N , T_L , $PAOD_L$, DR_L , and CR_L during both the daytime and nighttime are expressly examined. The main findings of the current study are:

1. The annual mean AOD_T values are slightly higher (~ 0.1) during the daytime compared to the nighttime. The highest values of AOD_T were observed during summer and the lowest values were observed during winter which suggested that summer is the most polluted season in Pakistan.
2. The higher annual mean values of N were observed over Punjab and Sindh, sequentially succeeded by Balochistan, Khyber-Pakhtunkhwa, Jammu-Kashmir, and Gilgit-Baltistan.
3. The H_L and H_H have shown a positive correlation with the elevation of the geographic location; i.e., higher the elevation, the higher the values of H_L and H_H , and negative correlation with the aerosol loadings; i.e., higher the values of H_L and H_H , less amount of aerosols in the atmosphere.
4. Aerosol particles exist at lower altitudes over Punjab and Sindh compared to the other regions of Pakistan.
5. A large number of aerosol amounts (AOD_L) is presented in the lowest aerosol layers over Punjab and Sindh compared to the other regions.
6. The annual mean values of AOD_L were observed higher during the nighttime than the daytime.
7. A large percentage of $PAOD_L$ was observed over the elevated area compared to the plain areas, however, aerosol particles over the elevated regions are less vulnerable to the public health due to higher values of H_L and less aerosol loadings.
8. A significant percentage of $PAOD_L$ during the nighttime compared to the daytime is more vulnerable to the public health in Punjab and Sindh due to a large amount of the aerosols in the lowest aerosol layer (AOD_L) as well as the lower altitude of the lowest aerosol layer (H_L).
9. More non-spherical nature of the aerosol particles was observed during the daytime compared to the nighttime in the following order: Balochistan > Gilgit-Baltistan > Sindh > Punjab, and Jammu-Kashmir. A large number of coarse-mode (large size particles) were observed over Punjab > Balochistan > Sindh > Gilgit-Baltistan > Jammu-Kashmir > Khyber-Pakhtunkhwa. Overall, a large number of coarse-mode non-spherical aerosols were presented during spring and summer compared to autumn and winter.

Overall, this research offers some scientific insights into the optical properties of the aerosols over Pakistan and this could help researchers and policymakers to mitigate air pollution issues and their effects on public health.

Author Contributions: Writing, M.Z. and B.S.; methodology, M.Z.; software, M.Z.; validation, G.H.; investigation, M.Z. and B.S.; review, M.B., L.A., M.U., Z.Q. and M.A.A.; project administration, M.Z.; funding acquisition, M.Z. All authors have read and agreed to the published version of the manuscript.

Funding: This research was funded by the National Natural Science Foundation of China (No. 41801282), Programs for Science and Technology Development of Henan Province (No. 192102310008), the Special Project of Jiangsu Distinguished Professor (1421061901001) by Jiangsu Department of Education, and the Startup Foundation for Introduction Talent of NUIST [grant number 2017r107].

Acknowledgments: We thank NASA for providing datasets of CALIPSO. We would also like to thank the editors for modifying and revising this manuscript.

Conflicts of Interest: The authors declare no conflict of interest.

References

1. Kaufman, Y.J.; Tanré, D.; Boucher, O. A satellite view of aerosols in the climate system. *Nature* **2002**, *419*, 215–223. [[CrossRef](#)] [[PubMed](#)]
2. Lelieveld, J.; Evans, J.S.; Fnais, M.; Giannadaki, D.; Pozzer, A. The contribution of outdoor air pollution sources to premature mortality on a global scale. *Nature* **2015**, *525*, 367–371. [[CrossRef](#)]

3. Pandolfi, M.; Cusack, M.; Alastuey, A.; Querol, X. Variability of aerosol optical properties in the Western Mediterranean Basin. *Atmos. Chem. Phys. Discuss.* **2011**, *11*, 8189–8203. [[CrossRef](#)]
4. Che, H.; Zhang, X.-Y.; Xia, X.; Goloub, P.; Holben, B.; Zhao, H.; Wang, Y.; Zhang, X.-C.; Wang, H.; Blarel, L.; et al. Ground-based aerosol climatology of China: Aerosol optical depths from the China Aerosol Remote Sensing Network (CARSNET) 2002–2013. *Atmos. Chem. Phys. Discuss.* **2015**, *15*, 7619–7652. [[CrossRef](#)]
5. Ramanathan, V.; Terborgh, J.; Lopez, L.; Núñez, P.; Rao, M.; Shahabuddin, G.; Orihuela, G.; Riveros, M.; Ascanio, R.; Adler, G.H.; et al. Aerosols, Climate, and the Hydrological Cycle. *Science* **2001**, *294*, 2119–2124. [[CrossRef](#)]
6. Menon, S.; Hansen, J.; Nazarenko, L.; Luo, Y. Climate Effects of Black Carbon Aerosols in China and India. *Science* **2002**, *297*, 2250–2253. [[CrossRef](#)]
7. Edenhofer, O.; Seyboth, K. Intergovernmental Panel on Climate Change (IPCC). *Encycl. Energy Nat. Resour. Environ. Econ.* **2013**, 48–56. [[CrossRef](#)]
8. Pandolfi, M.; Ripoll, A.; Querol, X.; Alastuey, A. Climatology of aerosol optical properties and black carbon mass absorption cross section at a remote high-altitude site in the western Mediterranean Basin. *Atmos. Chem. Phys. Discuss.* **2014**, *14*, 6443–6460. [[CrossRef](#)]
9. Bergin, M.; Cass, G.R.; Xu, J.; Fang, C.; Zeng, L.M.; Yu, T.; Salmon, L.G.; Kiang, C.S.; Tang, X.Y.; Zhang, Y.H.; et al. Aerosol radiative, physical, and chemical properties in Beijing during June 1999. *J. Geophys. Res. Space Phys.* **2001**, *106*, 17969–17980. [[CrossRef](#)]
10. Che, H.; Zhang, X.; Chen, H.; Damiri, B.; Goloub, P.; Li, Z.; Zhang, X.; Wei, Y.; Zhou, H.; Dong, F.; et al. Instrument calibration and aerosol optical depth validation of the China Aerosol Remote Sensing Network. *J. Geophys. Res. Space Phys.* **2009**, *114*, 03206. [[CrossRef](#)]
11. Dubovik, O.; Smirnov, A.; Holben, B.N.; King, M.D.; Kaufman, Y.J.; Eck, T.F.; Slutsker, I. Accuracy assessments of aerosol optical properties retrieved from Aerosol Robotic Network (AERONET) Sun and sky radiance measurements. *J. Geophys. Res. Space Phys.* **2000**, *105*, 9791–9806. [[CrossRef](#)]
12. Eck, T.F.; Holben, B.N.; Reid, J.S.; Dubovik, O.; Smirnov, A.; O'Neill, N.T.; Slutsker, I.; Kinne, S. Wavelength dependence of the optical depth of biomass burning, urban, and desert dust aerosols. *J. Geophys. Res. Atmos.* **1999**, *104*, 31333–31349. [[CrossRef](#)]
13. Zhang, M.; Liu, J.; Bilal, M.; Zhang, C.; Nazeer, M.; Atique, L.; Han, G.; Gong, W. Aerosol Optical Properties and Contribution to Differentiate Haze and Haze-Free Weather in Wuhan City. *Atmosphere* **2020**, *11*, 322. [[CrossRef](#)]
14. Zhang, M.; Ma, Y.; Gong, W.; Zhu, Z. Aerosol Optical Properties of a Haze Episode in Wuhan Based on Ground-Based and Satellite Observations. *Atmosphere* **2014**, *5*, 699–719. [[CrossRef](#)]
15. Che, H.; Xia, X.; Zhu, J.; Li, Z.; Dubovik, O.; Holben, B.; Goloub, P.; Chen, H.; Estelles, V.; Cuevas, E.; et al. Column aerosol optical properties and aerosol radiative forcing during a serious haze-fog month over North China Plain in 2013 based on ground-based sunphotometer measurements. *Atmos. Chem. Phys. Discuss.* **2014**, *14*, 2125–2138. [[CrossRef](#)]
16. Bilal, M.; Nichol, J.E.; Spak, S. A New Approach for Estimation of Fine Particulate Concentrations Using Satellite Aerosol Optical Depth and Binning of Meteorological Variables. *Aerosol Air Qual. Res.* **2017**, *17*, 356–367. [[CrossRef](#)]
17. Bilal, M.; Nichol, J.E.; Chan, P.W. Validation and accuracy assessment of a Simplified Aerosol Retrieval Algorithm (SARA) over Beijing under low and high aerosol loadings and dust storms. *Remote. Sens. Environ.* **2014**, *153*, 50–60. [[CrossRef](#)]
18. Magistrale, V. *Health Aspects of Air Pollution*; Springer Science and Business Media LLC.: Berlin/Heidelberg, Germany, 1992; pp. 25–31.
19. Kaiser, J. EPIDEMIOLOGY: How Dirty Air Hurts the Heart. *Science* **2005**, *307*, 1858b–1859b. [[CrossRef](#)]
20. Tie, X.; Wu, D.; Brasseur, G. Lung cancer mortality and exposure to atmospheric aerosol particles in Guangzhou, China. *Atmos. Environ.* **2009**, *43*, 2375–2377. [[CrossRef](#)]
21. Smirnov, A.; Holben, B.N.; Eck, T.F.; Slutsker, I.; Chatenet, B.; Pinker, R.T. Diurnal variability of aerosol optical depth observed at AERONET (Aerosol Robotic Network) sites. *Geophys. Res. Lett.* **2002**, *29*, 30–31. [[CrossRef](#)]
22. Omar, A.H.; Won, J.; Winker, D.; Yoon, S.; Dubovik, O.; McCormick, M.P. Development of global aerosol models using cluster analysis of Aerosol Robotic Network (AERONET) measurements. *J. Geophys. Res. Space Phys.* **2005**, *110*, 10–14. [[CrossRef](#)]

23. Bilal, M.; Nichol, J.; Nazeer, M. Validation of Aqua-MODIS C051 and C006 Operational Aerosol Products Using AERONET Measurements Over Pakistan. *IEEE J. Sel. Top. Appl. Earth Obs. Remote. Sens.* **2015**, *9*, 2074–2080. [[CrossRef](#)]
24. Bilal, M.; Nazeer, M.; Nichol, J.E.; Qiu, Z.; Wang, L.; Bleiweiss, M.P.; Shen, X.; Campbell, J.; Lolli, S. Evaluation of Terra-MODIS C6 and C6.1 Aerosol Products against Beijing, XiangHe, and Xinglong AERONET Sites in China during 2004–2014. *Remote. Sens.* **2019**, *11*, 486. [[CrossRef](#)]
25. Kleidman, R.G.; O'Neill, N.T.; Remer, L.A.; Kaufman, Y.J.; Eck, T.F.; Tanré, D.; Dubovik, O.; Holben, B.N. Comparison of Moderate Resolution Imaging Spectroradiometer (MODIS) and Aerosol Robotic Network (AERONET) remote-sensing retrievals of aerosol fine mode fraction over ocean. *J. Geophys. Res. Space Phys.* **2005**, *110*. [[CrossRef](#)]
26. Mishchenko, M.I.; Geogdzhayev, I.V.; Liu, L.; Ogren, J.; A Lacis, A.; Rossow, W.B.; Hovenier, J.W.; Volten, H.; Muñoz, O. Aerosol retrievals from AVHRR radiances: Effects of particle nonsphericity and absorption and an updated long-term global climatology of aerosol properties. *J. Quant. Spectrosc. Radiat. Transf.* **2003**, *79*, 953–972. [[CrossRef](#)]
27. Kosmopoulos, P.; Kaskaoutis, D.; Nastos, P.T.; Kambezidis, H. Seasonal variation of columnar aerosol optical properties over Athens, Greece, based on MODIS data. *Remote. Sens. Environ.* **2008**, *112*, 2354–2366. [[CrossRef](#)]
28. Chu, D.A.; Kaufman, Y.J.; Ichoku, C.; Remer, L.A.; Tanré, D.; Holben, B.N. Validation of modis aerosol optical depth retrieval over land. *Geophys. Res. Lett.* **2002**, *29*, 8007. [[CrossRef](#)]
29. Remer, L.A.; Kaufman, Y.J.; Ichoku, C.; Mattoo, S.; Chu, D.A.; Holben, B.; Dubovik, O.; Martins, J.V.; Li, R.; Tanré, D.; et al. Validation of MODIS aerosol retrieval over ocean. *Geophys. Res. Lett.* **2002**, *29*, MOD3-1–MOD3-4. [[CrossRef](#)]
30. Qiu, R.; Han, G.; Ma, X.; Xu, H.; Shi, T.; Zhang, M. A Comparison of OCO-2 SIF, MODIS GPP, and GOSIF Data from Gross Primary Production (GPP) Estimation and Seasonal Cycles in North America. *Remote Sens.* **2020**, *12*, 258. [[CrossRef](#)]
31. Zhang, M.; Liu, J.; Li, W.; Bilal, M.; Zhao, F.; Zhang, C.; Yuan, B.; Khedher, K.M. Evaluation of the Aqua-MODIS C6 and C6.1 Aerosol Optical Depth Products in the Yellow River Basin, China. *Atmosphere* **2019**, *10*, 426. [[CrossRef](#)]
32. Jethva, H.; Torres, O.; Ahn, C. Global assessment of OMI aerosol single-scattering albedo using ground-based AERONET inversion. *J. Geophys. Res. Atmos.* **2014**, *119*, 9020–9040. [[CrossRef](#)]
33. Zhang, M.; Wang, L.; Gong, W.; Ma, Y.; Liu, B. Aerosol Optical Properties and Direct Radiative Effects over Central China. *Remote Sens.* **2017**, *9*, 997. [[CrossRef](#)]
34. Winker, D.M.; Pelon, J. In The calipso mission, Geoscience and Remote Sensing Symposium. In Proceedings of the IEEE International, Toulouse, France, 21–25 July 2003.
35. Winker, D.; Vaughan, M.A.; Omar, A.; Hu, Y.; Powell, K.A.; Liu, Z.; Hunt, W.H.; Young, S. Overview of the CALIPSO Mission and CALIOP Data Processing Algorithms. *J. Atmos. Ocean. Technol.* **2009**, *26*, 2310–2323. [[CrossRef](#)]
36. Winker, D.M.; Pelon, J.R.; McCormick, M.P. The calipso mission: Spaceborne lidar for observation of aerosols and clouds. *Bull. Am. Meteorol. Soc.* **2010**, *91*, 1211–1229. [[CrossRef](#)]
37. Winker, D.; Hunt, W.H.; McGill, M.J. Initial performance assessment of CALIOP. *Geophys. Res. Lett.* **2007**, *34*, 228–262. [[CrossRef](#)]
38. Winker, D.; Tackett, J.L.; Getzewich, B.J.; Liu, Z.; Vaughan, M.A.; Rogers, R.R. The global 3-D distribution of tropospheric aerosols as characterized by CALIOP. *Atmos. Chem. Phys. Discuss.* **2013**, *13*, 3345–3361. [[CrossRef](#)]
39. Nichol, J.E.; Bilal, M. Validation of MODIS 3 km Resolution Aerosol Optical Depth Retrievals Over Asia. *Remote Sens.* **2016**, *8*, 328. [[CrossRef](#)]
40. Haq, Z.U.; Tariq, S.; Ali, M.; Mahmood, K.; Batool, S.A.; Rana, A.D. A study of tropospheric NO₂ variability over Pakistan using OMI data. *Atmos. Pollut. Res.* **2014**, *5*, 709–720. [[CrossRef](#)]
41. Ali, G.; Bao, Y.; Ullah, W.; Ullah, S.; Guan, Q.; Liu, X.; Li, L.; Lei, Y.; Li, G.; Ma, J. Spatiotemporal Trends of Aerosols over Urban Regions in Pakistan and Their Possible Links to Meteorological Parameters. *Atmosphere* **2020**, *11*, 306. [[CrossRef](#)]
42. Tariq, S.; Ali, M. Spatio-temporal distribution of absorbing aerosols over Pakistan retrieved from OMI onboard Aura satellite. *Atmos. Pollut. Res.* **2015**, *6*, 254–266. [[CrossRef](#)]

43. Shahid, M.Z.; Liao, H.; Li, J.; Shahid, I.; Lodhi, A.; Mansha, M. Seasonal Variations of Aerosols in Pakistan: Contributions of Domestic Anthropogenic Emissions and Transboundary Transport. *Aerosol Air Qual. Res.* **2015**, *15*, 1580–1600. [[CrossRef](#)]
44. Alam, K.; Iqbal, M.J.; Blaschke, T.; Qureshi, S.; Khan, G. Monitoring spatio-temporal variations in aerosols and aerosol–cloud interactions over Pakistan using MODIS data. *Adv. Space Res.* **2010**, *46*, 1162–1176. [[CrossRef](#)]
45. Zhang, M.; Liu, J.; Bilal, M.; Zhang, C.; Zhao, F.; Xie, X.; Khedher, K.M. Optical and Physical Characteristics of the Lowest Aerosol Layers over the Yellow River Basin. *Atmosphere* **2019**, *10*, 638. [[CrossRef](#)]
46. Begum, B.A.; Biswas, S.K.; Pandit, G.G.; Saradhi, I.V.; Waheed, S.; Siddique, N.; Seneviratne, M.S.; Cohen, D.; Markwitz, A.; Hopke, P.K. Long-range transport of soil dust and smoke pollution in the South Asian region. *Atmos. Pollut. Res.* **2011**, *2*, 151–157. [[CrossRef](#)]
47. Alam, K.; Qureshi, S.; Blaschke, T. Monitoring spatio-temporal aerosol patterns over Pakistan based on MODIS, TOMS and MISR satellite data and a HYSPLIT model. *Atmos. Environ.* **2011**, *45*, 4641–4651. [[CrossRef](#)]
48. Milroy, C.; Martucci, G.; Lolli, S.; Loaec, S.; Sauvage, L.; Xueref-Rémy, I.; Lavrič, J.V.; Ciais, P.; Feist, D.G.; Biavati, G.; et al. An Assessment of Pseudo-Operational Ground-Based Light Detection and Ranging Sensors to Determine the Boundary-Layer Structure in the Coastal Atmosphere. *Adv. Meteorol.* **2012**, *2012*, 1–18. [[CrossRef](#)]
49. Bilal, M.; Nichol, J.E.; Bleiweiss, M.P.; Dubois, D. A Simplified high resolution MODIS Aerosol Retrieval Algorithm (SARA) for use over mixed surfaces. *Remote Sens. Environ.* **2013**, *136*, 135–145. [[CrossRef](#)]
50. Stull, R.B. *An Introduction to Boundary Layer Meteorology*; Springer: Berlin/Heidelberg, Germany, 1988.
51. Ranjan, R.R.; Ganguly, N.D.; Joshi, H.P.; Iyer, K.N. Study of aerosol optical depth and precipitable water vapour content at rajkot, a tropical semi-arid station. *Indian J. Radio Space Phys.* **2007**, *36*, 27–32.
52. Sarkar, S.; Chokngamwong, R.; Cervone, G.; Singh, R.; Kafatos, M. Variability of aerosol optical depth and aerosol forcing over India. *Adv. Space Res.* **2006**, *37*, 2153–2159. [[CrossRef](#)]
53. Alam, K.; Blaschke, T.; Madl, P.; Mukhtar, A.; Hussain, M.; Trautmann, T.; Rahman, S. Aerosol size distribution and mass concentration measurements in various cities of Pakistan. *J. Environ. Monit.* **2011**, *13*, 1944. [[CrossRef](#)] [[PubMed](#)]
54. Eck, T.F.; Holben, B.N.; Ward, D.E.; Dubovik, O.; Reid, J.S.; Smirnov, A.; Mukelabai, M.M.; Hsu, N.C.; O'Neill, N.T.; Slutsker, I. Characterization of the optical properties of biomass burning aerosols in Zambia during the 1997 ZIBBEE field campaign. *J. Geophys. Res. Space Phys.* **2001**, *106*, 3425–3448. [[CrossRef](#)]
55. Reid, J.S.; Eck, T.F.; Christopher, S.; Hobbs, P.V.; Holben, B. Use of the Ångström exponent to estimate the variability of optical and physical properties of aging smoke particles in Brazil. *J. Geophys. Res. Space Phys.* **1999**, *104*, 27473–27489. [[CrossRef](#)]
56. Reid, J.S.; Lagrosas, N.D.; Jonsson, H.H.; Reid, E.A.; Atwood, S.A.; Boyd, T.J.; Ghatge, V.P.; Xian, P.; Posselt, D.J.; Simpas, J.B. Aerosol meteorology of maritime continent for the 2012 7seas southwest monsoon intensive study—Part 2: Philippine receptor observations of fine-scale aerosol behavior. *Atmos. Chem. Phys.* **2016**, *16*, 14057–14078. [[CrossRef](#)]
57. Ali, M.; Tariq, S.; Mahmood, K.; Daud, A.; Batool, A.; Haq, Z.U. A study of aerosol properties over Lahore (Pakistan) by using AERONET data. *Asia Pac. J. Atmos. Sci.* **2013**, *50*, 153–162. [[CrossRef](#)]
58. Zhang, M.; Wang, L.; Bilal, M.; Gong, W.; Zhang, Z.; Guo, G. The Characteristics of the Aerosol Optical Depth within the Lowest Aerosol Layer over the Tibetan Plateau from 2007 to 2014. *Remote Sens.* **2018**, *10*, 696. [[CrossRef](#)]

